International Journal of Fluid Power, 2014
Vol. 15, No. 3, 169–180, http://dx.doi.org/10.1080/14399776.2014.976097

Taylor & Francis
Taylor & Francis Group

Procedure for hydraulic oil heat exchanger performance improvement through integrated CFD analysis

R. Paoluzzi*, A. Bonanno, C. Ferrari and M. Martelli

C.N.R. – IMAMOTER Institute for Agricultural and Earth Moving Machines, National Research Council of Italy, Via Canal Bianco 28, 44124, Ferrara, ITALY

(*Received 14 August 2014; accepted 9 October 2014*)

Present and future constraints on the layout of hydraulic circuits onboard mobile machinery will require more and more compact components with improved efficiency. The need to use IC engines complying with new standards on emissions will introduce new components into the engine hood, like Exhaust Gas Recirculation (EGR), Selective Catalytic Reduction (SCR), Dust Particulate Filter (DPF) and more, reducing the space available for components where traditionally the ratio between dimension and performance was not considered a 'hard boundary' to the design space. One of the components of the hydraulic circuit affected by the general tendency to an increase of the operating temperatures due to the new-generation engines introduction is the heat exchanger. The need to design properly tailored, efficient and compact heat exchangers is therefore one of the first priority targets in machine design. Accurate and reliable estimate of the performance at the design stage is a priority as well.

This paper shows how the concurrent use of Computational Fluid Dynamics (CFD) and numerical approximations allow the performance prediction with a good correlation with the experimental results. The approach is applied to a cross-flow heat exchanger and is aimed at developing a software tool able to predict the global performance, yet being easily applicable to a wider range of cases. The approach used and described in this paper can be easily extended to a product set, variable in both dimension and technical characteristics. The key feature is to split the exchanger into sub-domains having homogeneous boundary conditions on either side, hot and cold, in order to estimate their performance in terms of WHTC (Wall Heat Transfer Coefficient) and pressure drop. This step applies a detailed CFD analysis. Results obtained are used as building blocks in a dedicated software tool developed at IMAMOTER-C.N.R. which sums-up the results to full scale. This approach features a reliable, yet flexible, evaluation of the exchanger performance under different environmental conditions and dimensions. The results obtained by the numerical analysis have been compared with experimental tests, showing the good degree of approximation achieved.

Keywords: heat exchanger; software; performance evaluation; CFD; sub-domain; η-NTU

1. Introduction

Many authors studied the problem of cross flow heat exchangers in recent years. Navarro and Cabeza-Gomez (2005) studied different analysis methodologies of thermal exchanger, based on 'elements' radiator subdivision, in which the thermal equations are algebraically calculated and the results are then combined in order to obtain the global performances in term of ε-NTU (Number of Transfer Units). A similar methodology is presented in a paper written by G.L. Zarotti (1998) in 1998. Kim et al. (2001) highlighted the importance of inclination angle from the vertical position on the air-side thermal hydraulic performance for a multi-louvered fin and flat tube heat exchanger. Different type of Computational Fluid Dynamic (CFD) codes and approaches have been used to evaluate the pressure drop, the uneven flow distribution and the thermal field (Aslam Bhutta et al. 2012), demonstrating that CFD is an effective tool for predicting the behaviour and performance of a wide variety of heat exchangers. Also the importance of fin efficiency was highlighted, since an incorrect flow distribution significantly lowers the heat exchanger global efficiency. Prasad (1997) developed a rating algorithm and other authors performed many studies of heat exchangers using CFD techniques in order to achieve radiators optimization (Wen et al. 2006, Ismail et al. 2009, Zhang 2009, Zhang et al. 2010). The optimal number of passes for a fixed size heat exchanger has been studied by Kim et al. (2008), improving the radiator performance compared to a reference. Some recent papers approached the possibility to use genetic algorithms to search, combine and optimize the structure and size of compact heat exchanger (Hilbert et al. 2006, Xie et al. 2008, Najafi et al. 2011). It is worth noting, in addition, the possibility to use non-conventional materials (e.g. metallic foam) to explore new ways to improve heat exchanger performance (T'Joen et al. 2010). Available information in scientific literature provide various theories and analytical models, but experimental, or application data, are difficult to be applied to different geometries. The natural consequence is that design is mostly based on the use of numerical correlations sometimes relying on highly empirical assumptions.

*Corresponding author. Email: r.paoluzzi@imamoter.cnr.it

© 2014 Taylor & Francis

The correlations change as a function of geometry and manufacturing process, this makes the fins study complex, and dedicated studies for every different fin architecture are therefore necessary.

Scientific literature seems lacking in examples on comparative studies of different fins integrated in a specific general check context in order to drive the design process, or at least to give a reference frame of evaluation. The aim of this paper is to show a methodology which, starting from a fluid-dynamic study, makes possible to economically and efficiently design radiators which are easily adaptable to the widest possible range of operating conditions. The methodology was implemented in a software tool developed at IMAMOTER-C.N.R. and validated by experimental third party tests.

2. Procedure outline

The path towards a comprehensive predictive evaluation of the heat exchanger performance can rely on three main design options:

- Use of closed-form analytical models, based on theoretical models adapted to nearly real geometries;
- Integrated thermal and fluid dynamic analysis of the three domains (hot fluid, cold fluid and solid) at full scale;
- Decoupling of the domains (hot fluid and cold fluid) with solution based on the continuity of the boundary values of the variables at domain interfaces.

The first option, though based on years of experience and experimental studies, has the drawback of an unknown confidence level when new geometries of the flow channels and fins are considered. The second, yet based on solid numerical techniques, has the drawback of model complexity and computational power required, and moreover is limited to one single physical case per application. The third is aimed at reducing the computational demand and geometric complexity, but again has an application limited to a single geometry and size of the heat exchanger.

The procedure proposed in the paper, based on the modular decomposition of heat exchanger blocks, is aimed at providing a solution which retains the detail level of a fully coupled analysis and allows the extension of the results to a wide range of heat exchanger sizes. It also allows a reasonably easy evaluation of the effect of geometry changes in the design of individual fins and channel geometry, on both hot and cold side of the heat exchanger.

The basic idea is to simulate the full exchanger[1] using partitioned sub-domains, considered as a combination of elements with series and parallel layout. The heat exchanger is decomposed (Figure 1) in portions, where the flow has common peculiar characteristics (mainly from the point of view of boundary conditions applied). The exchanger can be split into nine different sub-domain categories:

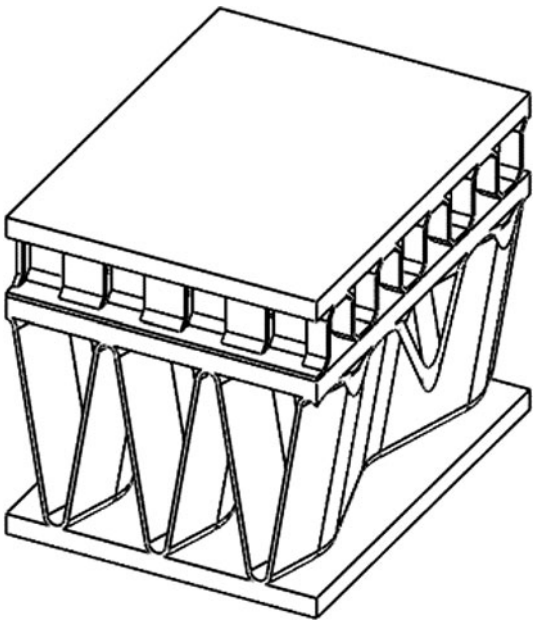

Figure 1. Example of geometry of a heat-exchanger portion for coupled (hot-cold flow) simulation.

- Number 1: has an inlet boundary condition for both fluids; different singularities (i.e. edges), causing turbulence, are present; both flows come from a plenum and go inside the radiator;
- Number 2: features inlet boundary condition for the cooling flow, whereas the hot flow has a completely developed motion (no border effects)
- Number 3: is similar to No. 1, with the remarkable difference that hot flow has an outlet boundary condition;
- Number 4: the hot flow has an inlet boundary condition, and the cooling flow can be considered as fully developed;
- Number 5: is an inner domain; both flows are fully developed;

The other sub-domains are a permutation of the previous ones. Summarizing, the sub-domains 1-2-3-4-6-7-8-9 have one or more plenum attached to them; the sub-domain 5 (inner domain) does not (Figure 2).

Each sub-domain can be solved with a fully coupled thermal-fluid analysis with a reasonably low computational power demand and proper mesh refinement. The basic idea is to build-up a lookup table of performance of the individual sub-domains as a function of: fluid flow rates, wall boundary temperatures, fluid temperatures. The performance indicator used is the WHTC (Wall Heat Transfer Coefficient). A pressure drop in fluid flow calculation is possible as well.

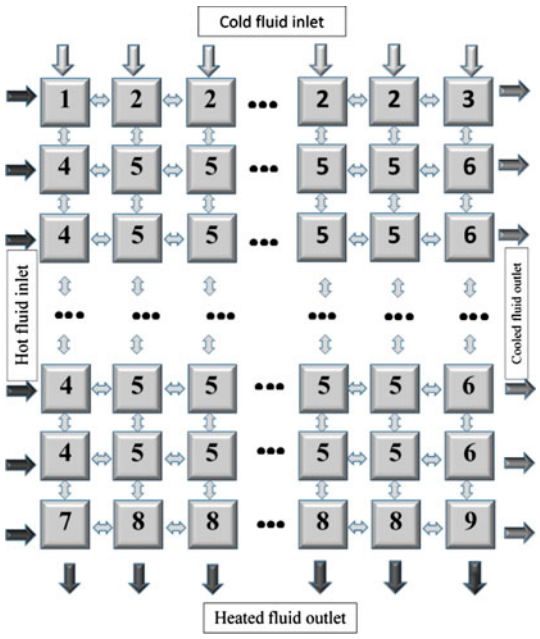

Figure 2. Heat exchanger schematic view.

$$WHTC = \mathfrak{F}(T_h, T_c, Q_h, Q_c, T_w)$$

Where subscripts h, c and w refer to hot, cold flow and wall, respectively.

Boundary elements are subject to physical constraints coming from the external environment (i.e. available flow rates, ambient temperature), internal elements must satisfy the continuity of variables at the interface with neighbour elements. The inner sub-domain ($S_{i,j}$) exchanges variables with the four neighbours, and application of continuity constraints to the interfaces allow the propagation of the solution inside the domain. The originality of the approach is that this step is not performed altering the boundary conditions of CFD runs. It uses the performance maps developed with the CFD mapping of each sub-domain and requires only minimal computational effort to solve systems of algebraic equations.

Once a global solution is obtained, the knowledge of the global WTHC allows the estimation of the overall thermal power exchanged. An estimation of the overall pressure drop in fluid flow, simply comes from the summation of individual contributions.

3. Case Study

In this case study, the heat exchanger considered is: air-air (four geometries), air-oil (two geometries) or air-water (two geometries).

The cold (coolant) fluid is always air (geometries from A0 to A4), the hot fluid (cooling) could be air (geometries P1 and P3), oil or water (geometries P0 and P1 for both fluids). The cold fluid fins have pseudo-sinusoidal geometry with rectangular or trapezoidal section. The hot fluid fins have a wavy geometry with a more complex offset (Figure 3).

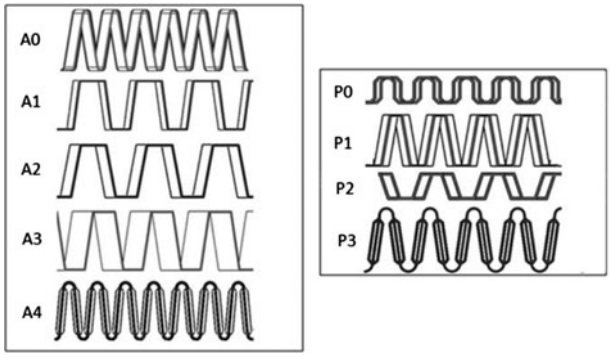

Figure 3. Geometric examples of tested fins.

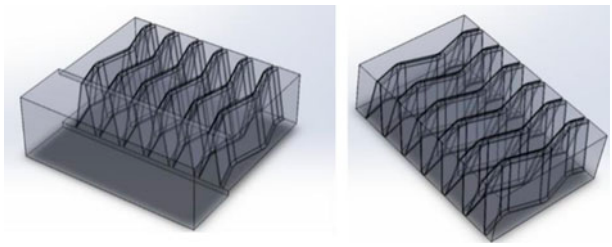

Figure 4. Examples of sub-domain geometries with and without plenum.

ANSYS-CFX^{TM}v 14.0, was used for CFD simulations. The code uses a finite volumes approach and, due to the complexity of the geometry, the mesh construction requires particular care, in order to achieve good discretization of the near-wall laminar layers and to adequately predict the heat exchange and pressure drop values.

3.1. CFD problem layout

A first problem faced was the decision to keep the domain fully coupled or to adopt, even in this case, the decoupling of hot and cold fluid flow. To this purpose a series of numerical runs comparing the two approaches have been performed, and show that, provided that the decoupling is made at the solid interface, and that the thermal energy exchanged at the interface is used as solution constraint, the difference between a fully coupled approach and a decoupled computation is negligible. It was therefore decided to adopt, for each sub-domain, a decoupled approach according to the above mentioned strategy.

A further set of preliminary analysis gave the evidence of a substantial independency of the results with the flow direction: the heat exchange coefficient and the pressure drop do not show variation with the plenum fins flow direction.

Taking into account these preliminary results, where the sub-domains responsible of a WHTC variation and having this characteristic are only of type 2 and type 5, the problem was simplified accordingly. This simplified

layout was used to characterize four hot fluid fins (from P1 to P3), which have the role to cool down the working fluid (i.e. oil), and five cold fluid fins (from A0 to A4). The three working fluids considered are hydraulic oil (Arnica 46), a water-glycol mixture (50/50) and air.

3.2. Geometry and mesh construction

A detailed 3-D solid model of the geometry was the starting point of the mesh construction. Table 1 presents the dimensions of the different domains, compatible with the contrasting needs of adequate average solution and subsequent CFD model size.

According to the reference system used (Figure 5) the length of the cold fin sub-domain is equivalent to the width of the hot sub-domain, allowing a proper mapping of cross flow. The dimension in the Z direction of the P1-P3 geometries should be as close as possible to the dimension in the X direction of the A0-A4 geometries, and vice versa.

All the geometry features considered not relevant have been simplified during the modelling phase with a combination of automatic (defeaturing) and manual modifications.

This phase requested a particular attention because the heat exchange phenomenon is sensible to near-wall velocity field. For this reason it is necessary to generate a mesh able to adequately catch the velocity gradient normal to the wall surface, limiting the need to adopt specialized wall functions. The solution applied in this work is to use an inflated boundary (Figure 6) with five exahedric elements layers near the sub-domains walls. The resulting unstructured mesh elements number is relatively high (some 7.0 × 10^6), but gives the possibility to reach a good global solution accuracy and adequate precision in the near-wall region.

Table 1. Dimension [mm] of different sub-domains.

Type	X [mm]	Y [mm]	Z [mm]
A0	22.00	10.00	33.64
A1	22.00	10.00	31.23
A2	22.00	8.00	35.86
A3	22.00	10.00	36.80
A4	22.00	10.00	31.00
P0	34.06	3.00	22.50
P1	26.00	6.00	21.70
P2	31.25	3.00	21.66
P3	33.00	7.05	21.00

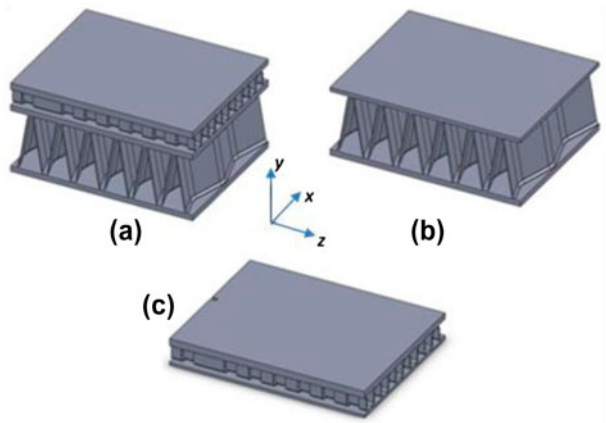

Figure 5. Example of sub-domain geometry; (a) traditional analysis with coupled sub-domain; (b) and (c) split sub-domain for new approach simulation.

3.3. Boundary conditions and simulation strate

The correctness of boundary condition set-up is a key factor in every simulation study. This work assumes the temperature of the fin surface as a constant. The smaller the computational domain dimensions the better this approximation holds. Other boundary conditions used in the sub-domain simulation are:

- Inlet with imposed temperature and velocity;
- Outlet at 0 relative pressure (with atmospheric reference);[2]
- Symmetry condition between the neighbour sub-domains

Different temperatures and velocities have been used in order to map expected operating conditions according to the principle presented in paragraph 2 (Table 2).

The numeric solution was obtained using the k-ωturbulence model, with wall scalable conditions; the Navier-Stokes computation method was set up on first

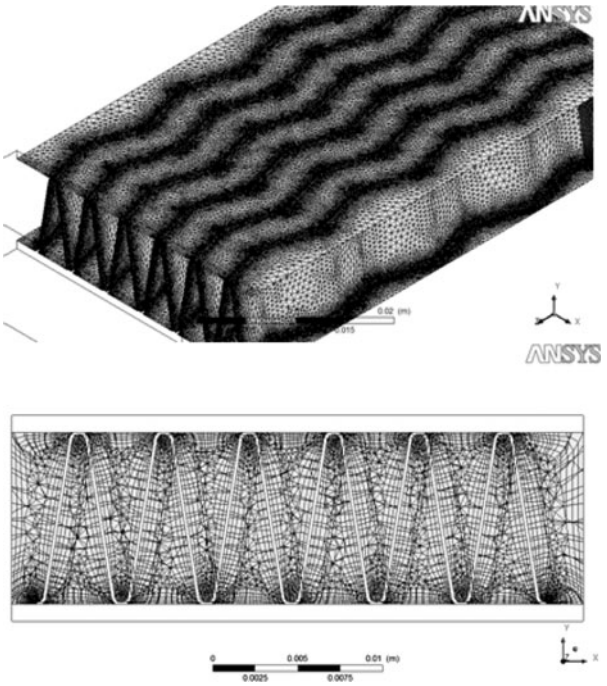

Figure 6. Mesh with inflated boundary.

Table 2. Operational points considered in the CFD simulations.

Type	Temperature (°C)	Velocity (m/s)
A0-A4	20	4.0; 8.0; 12.0
	40	
	50	
P0-P2 (Water)	85	0.2; 0.8; 1.2
	95	
	105	
P0-P2 (Oil)	60	0.2; 0.8; 1.2
	80	
	90	
P1-P3(Air)	120	2.0; 4.0; 8.0
	160	
	200	

order with high resolution; the convergence was set at RMS residual value of 5×10^{-05}.

3.4. Sub-domains result

The CFD analysis gave information on the WHTC and the pressure drop of different sub-domains. For the sake of generalization, the results are presented in graphic format and normalized to their maximum value. Figure 7 reports the results at the hot fluid fin (P0) for three different inlet velocities and temperatures.

The use of a 3 × 3 matrix of result allows the construction of the performance maps with an optimal trade-off between resolution and computational power required. The results were obtained and mapped for all the combinations applicable to the study.

4. Application of the method

4.1. The heat exchanger mapping

According to the proposed principle, the heat exchanger was conceived as a sub-domain cluster having common fluid dynamic characteristics (Figure 8). The CFD simulations performed on the sub-domains gave the WHTC and Δp as functions of fluid temperature and velocity.

The fins layers number is given by:

$$N_{Fl} = \frac{\left[H_e - H_f - (2 * H_s)\right]}{H_f + H_t + 1.6} + 1 \quad (1)$$

Where the *side* is the separation element between the fin layer and the channel layer, used to separate the different fluids; the term *1.6* is the thickness (in mm) of two sheets used (0.8 mm each) to seal the fin layers at the upper and lower side. The term *+1* is needed to take into account that the heat exchanger starts and ends always with a fin layer. The number of channels can be derived starting from the number of fin layers:

$$N_{Tl} = N_{Fl} - 1 \quad (2)$$

After having defined the number of layers, it is necessary to compute the number of 'slices'. This is the number of repetitive sections, each one made by the set of fins and channels calculated above:

$$N_{sF} = \frac{D_e - 2 * L_{sF2}}{L_{sF5}} \quad (3)$$

$$N_{sT} = \frac{W_e - 2 * L_{sT2}}{L_{sT5}} \quad (4)$$

The WHTC and Δp of fin and channel sub-domains at specified values of temperature and velocity come as a result from the performed CFD computations. For example, considering the channel P0 and P2, the sub-domain performance with an oil velocity of 0.2 – 0.8 – 1.2 m/s and a temperature of 60 – 80 – 90 °C was mapped. The matrix of velocity-temperature data was further interpolated using a cubic spline approach.

The cubic spline interpolation was selected because of its ability to provide smooth, yet reliable, interpolation. It provided the expected values of WHTC and Δp as a function of temperature and velocity of considered flow.

The WHTC of a generic sub-domain, is given by CFD results (Table 3) at the imposed operating conditions reported in Table 4.

From these results three splines can be derived, each one for a given velocity. They give the heat exchanger coefficient as a function of temperature.

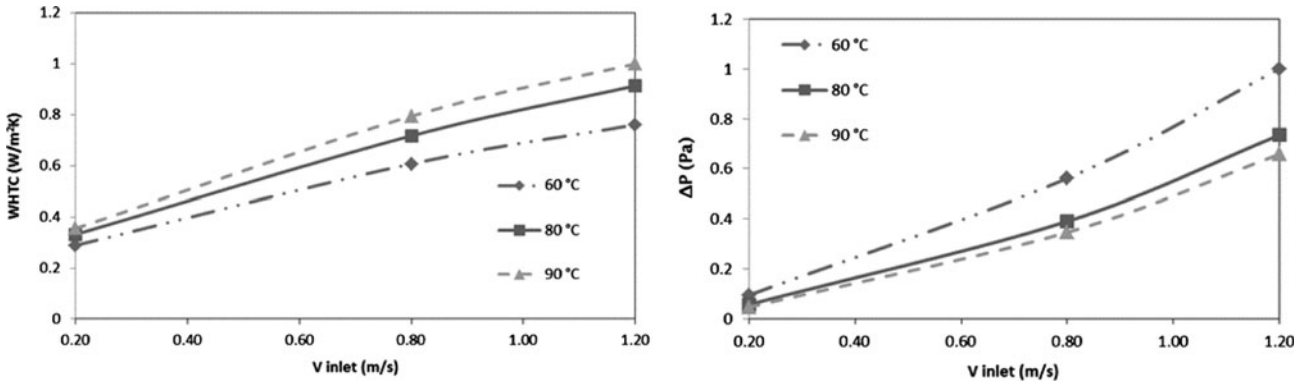

Figure 7. Normalized WHTC and δp of one of tested geometries.

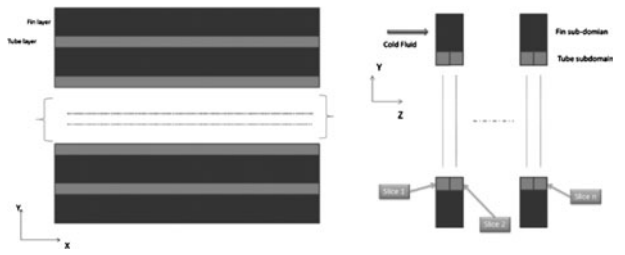

Figure 8. Heat exchanger schematization (left–frontal view; right–lateral view) with fins and channels subdivision.

Table 3. WHTC at different fluid temperature and velocity obtained by CFD analysis.

	Fluid velocity [m/s]		
Fluid Temperature [°C]	4	8 WHTC [W/m^{2}K]	12
20	76.67	127.46	172.67
40	73.14	121.50	157.40
50	71.52	118.64	150.10

Table 4. Hot and cold fluid flow rate applied in the experimental tests.

Hot fluid flow rate (l/min)	Cold fluid flow rate (m^3/h)
56	1700
	3500
	6000
70	1700
	3500
	6000
84	1700
	3500
	6000

Three different WHTC values for a given T_m temperature (the average temperature between the T_{IN} and the T_{OUT} of the generic sub-domain) can be obtained (Figure 9).

These three points define a new spline, which gives WHTC variation at a given temperature T_m, as a function of velocity (Figure 10).

The knowledge of the fluid average velocity in a sub-domain allows the use of the interpolating curves to obtain the WHTC and Δp at fluid temperature T_m and velocity v_m (Figure 11).

This calculation is repeated for each and every sub-domain. A lookup table for WHTC as function of temperature and velocity can therefore be obtained and mapped (Figure 12). The procedure to calculate the pressure drop for sub-domains Δp@(T_m; v_m) is similar.

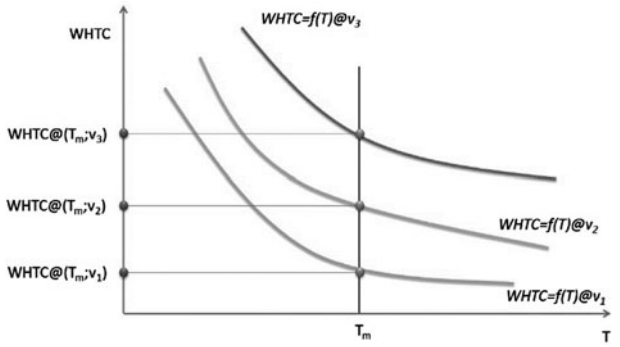

Figure 9. Extrapolated WHTC values from the splines.

Figure 10. Cubic spline of the WHTC as a function of velocity for a given temperature t_m.

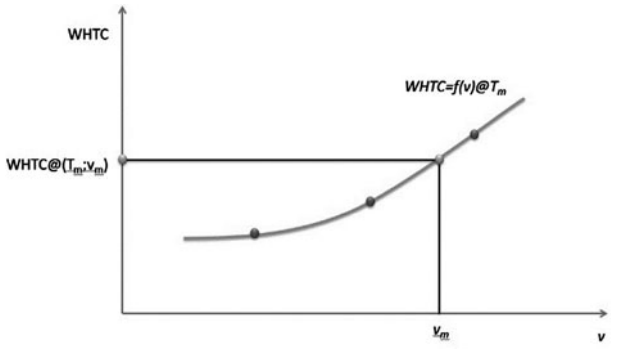

Figure 11. WHTC of the give sub-domain at temperature t_m and velocity v_m.

4.2. *Procedure to calculate the exchanged power*

The calculation of the exchanged power is based on the standard (η-NTU) method. The main relationships used are:

$$Z = \frac{\rho_H C_H Q_H}{\rho_C C_C Q_C} \tag{5}$$

$$\frac{1}{h_e} = \frac{1}{h_H} + \frac{1}{h_C \frac{S_C}{S_H}} \tag{6}$$

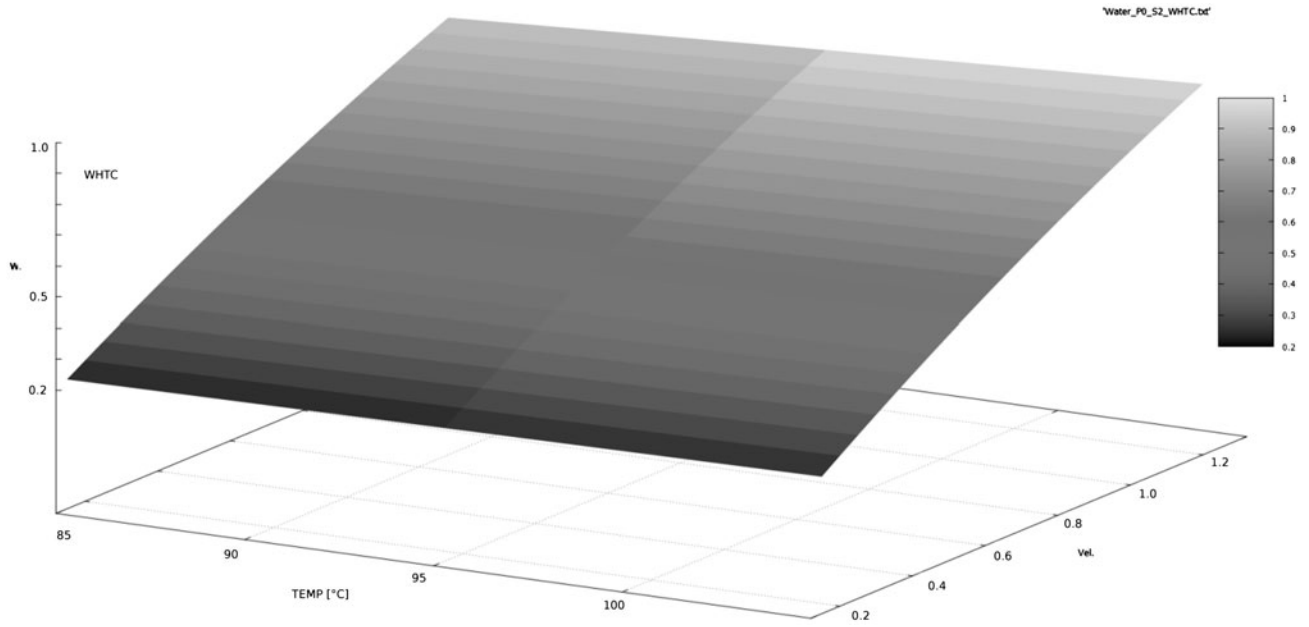

Figure 12. Normalized map of WHTC as a function temperature and fluid velocity.

$$NTU = \frac{h_e S_H}{\rho_H c_H Q_H} \tag{7}$$

$$\eta = \frac{NTU}{\left(\frac{NTU}{1 - e^{-NTU}}\right) + \left(\frac{zNTU}{1 - e^{-zNTU}}\right) - 1} \tag{8}$$

These equations are generally used to calculate the heat exchanged by the full radiator. In this approach, they were applied at *module* level, where the *module* is an element made by a fin sub-domain and a channel sub-domain as explained in Figure 13.

The hot fluid flow rate (Q_H) goes into the first module with a temperature T_1, a density ρ_1 and a heat capacity C_1 and flows out with a temperature T'_2 , a density ρ'_2 and a specific heat capacity C'_2. Similarly the cold fluid flow rate (Q_C) goes into the first module with a temperature T_3, a density ρ_3 and a specific heat capacity C_3 and flows out with a temperature T'_4, a density ρ'_4 and a specific heat capacity C'_4. The hot fluid OUT temperature, density and specific heat capacity from the first module is now the IN temperature of the second module ($T'_2 = T''_1$; $\rho'_2 = \rho''_1$; $C'_2 = C''_1$). In our system, NTU, Z, T_1, and T_3 are known, the unknown terms are T_2 and T_4, which can be calculated using the following equations:

$$T_2 = T_1 - \eta(NTU, Z) * (T_1 - T_3) \tag{9}$$

$$T_4 = T_3 - Z * (T_1 - T_2) \tag{10}$$

The wall heat transfer coefficients h_C and h_H are estimated using the introduced cubic spline interpolation. The hot and cold fluid densities are computed as average

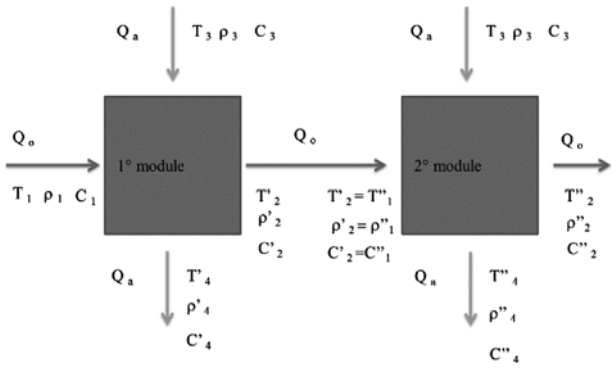

Figure 13. Schematization of the calculation method.

value considering the IN and OUT sub-domain temperatures. The program iterates until, for every module, the following condition is satisfied:

$$\rho_H C_H Q_H (T_1 - T_2) = \rho_C C_C Q_C (T_4 - T_3) \tag{11}$$

The output temperature of the hot fluid (the same applies for the cold fluid) will be different for every slice. This is because the first slice of hot fluid will cross a colder air flow compared to the second slice. This holds until the last slice (Figure 14). It implies that, in spite of the assumption that the hot fluid input temperature is considered constant, the output temperature will be different for every slice.

To account for this effect, the software calculates an average output temperature, for both cold and hot fluid, using the standard equation of exchanged thermal power:

$$H = \rho Q C_p \Delta T \tag{12}$$

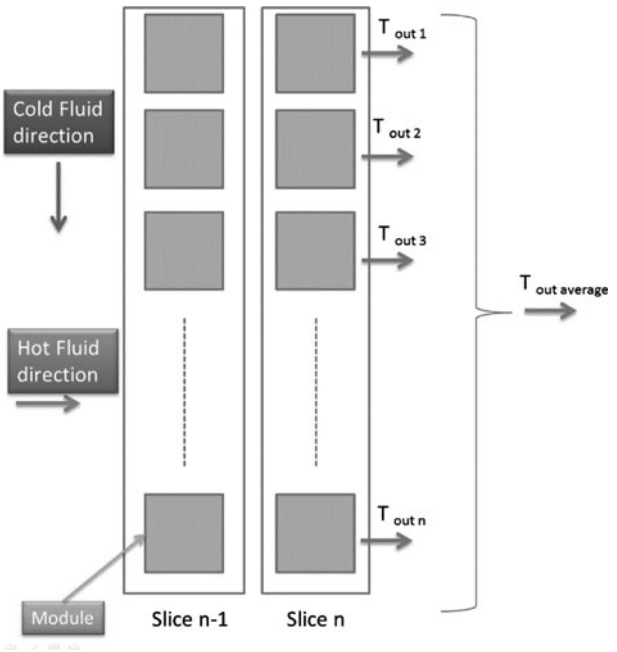

Figure 14. Schematization of output temperature estimation.

Where H is the exchanged thermal power,ρ is the fluid density, C_p is the constant pressure-specific heat, Q the relevant flow rate and ΔT the temperature difference.

Once the net exchanged power is computed, as sum of individual modules contribution, and considering an average density $\rho_{average}$ and an average constant pressure specific heat $C_{p\text{-}average}$ as temperature function, it is possible to write:

$$T_{out} = T_{in} + \frac{H}{\rho_{average} Q C_{p-average}} \tag{13}$$

4.3. Calculation of the pressure drop

The pressure drop is estimated following the same procedure used in the previous paragraph. Three different splines are generated, representing Δp as a function of temperature at three different velocity values. Three different points (Figure 15a), considering a generic temperature T_m which show the pressure drop at temperature T_m and velocity v_1, v_2, v_3, are obtained and used to calculate a second spline (Figure 15b) showing the pressure drop as a function of velocity for a given temperature.

The whole pressure drop is obtained by simple summation.

$$\Delta p_{total} = \sum \Delta p_{modules} \tag{14}$$

5. Experimental results

Experimental tests have been carried out at the Industrial Engineering Department of the University of Bergamo (Italy) in order to assess the confidence level of data obtained using the process described in this paper (Caratterizzazione a banco delle prestazioni di radiatori aria-acqua 2012). The procedure used is in accordance with ISO 5801:2007 standard requirements (ISO 5801:2007). Only the water-air heat exchangers were tested due limitations imposed by the test rig layout. Two different cold fluid fin geometries have been tested: one with a geometry developed to avoid the dust clogging (Low Clogging: LC) and another one with a geometry aimed at improving the performance (High Performance: HP). The channels geometry was the same for both radiators tested (P0). The tests used three different values of hot and cold flow rates, getting a total amount of nine different test conditions as shown in Table 4.

The experimental apparatus schematics are shown in Figure 16. It included a tunnel for air flow stabilization and an instrumented panel for air flow rate measurement. All data were acquired using NI DAQ AT-MIO-64E-3 in LabView®. Sensors used were: PT100 Platinum thermocouples with a precision of ±0.375°C@50°C; electromagnetic flow rate sensor Endress & Hauser Promag 30 F, 0-12.6 l/s, ±0,5%, differential pressure sensors Endress & Hauser PMD 235, 0-100 kPa, ±0.1%.

Due to the confidentiality requested by the industrial partner in this research, only the relative errors between numerical and experimental results are shown in Figures 16 to 20. Figure 17 presents the percentage difference between numerical and experimental exchanged power at a given cold fluid flow rate and different hot fluid flow

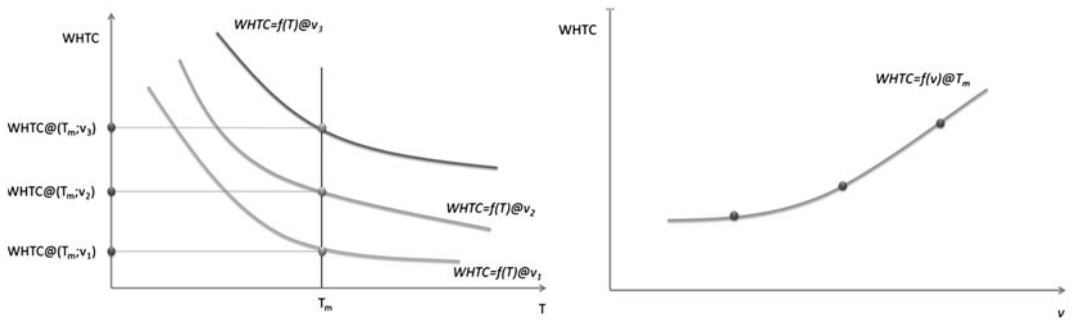

Figure 15. Spline used to calculate the pressure drop for a give velocity and temperature (t_m; v_m).

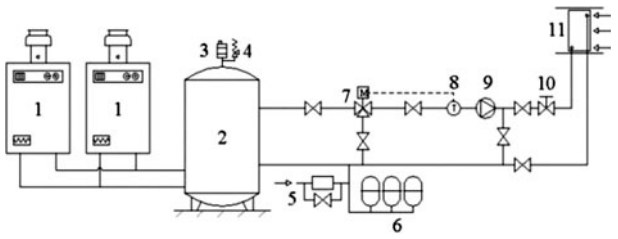

Figure 16. Hydraulic circuit for test: 1- boilers, 2 - hot water reservoir, 3 - drain, 4 - safety valve, 5 - manual feeding, 6 - expansion volumes, 7 -three-way valve, 8 - temperature sensor, 9 - recirculation pump, 10 - flow control valves, 11 - heat exchanger.

rate: the correlation between the experimental and calculated results is quite good, the maximum percentage difference is 5% for HP geometry and less than −10% for LC geometry. At higher water flow rates the software becomes more precise and starts to slightly underestimate the experimental results. Figure 18 shows the percentage difference between the hot fluid pressure drop at different flow rates: in this case an overestimation ranging from 35% (low flow rate – LC geometry) to 13% (high flow rate – HP geometry) compared to the experimental results is found and will be discussed in paragraph 6.

Figure 19 shows the percentage differences of output temperature for hot fluid. In this case the calculated results appear in remarkably good correlation compared to the experimental data. The maximum relative error is lower than 4.5% for HP geometry and not larger than 0.4% for LC geometry.

Figure 20 shows percentage differences between the calculated and experimental cold fluid pressure drop. In this case, a discrepancy between the results referred to the HP fins and those to the LC geometry is noted and will be discussed in paragraph 6 as well. The software overestimates the HP case (12% at low flow rate, 26% at high flow rate); on the contrary, in the LC case, the correlation is poor at lower flow rate (lower than 16%) and remarkably good at high flow rate (less than 2%).

This is symptomatic of a need for criticism on results in the CFD analysis on the high performance fins geometry, especially at high flow rate of cold fluid.

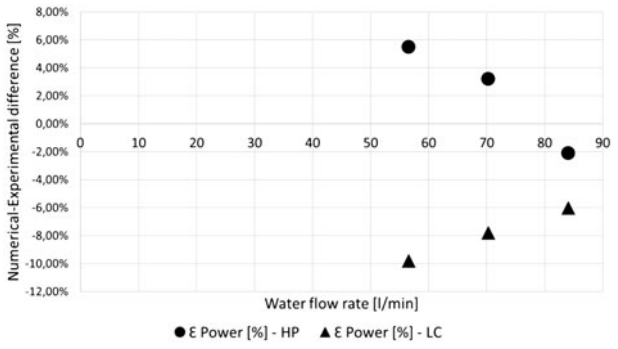

Figure 17. Percentage difference between numerical and experimental exchanged power at different cold fluid flow rates.

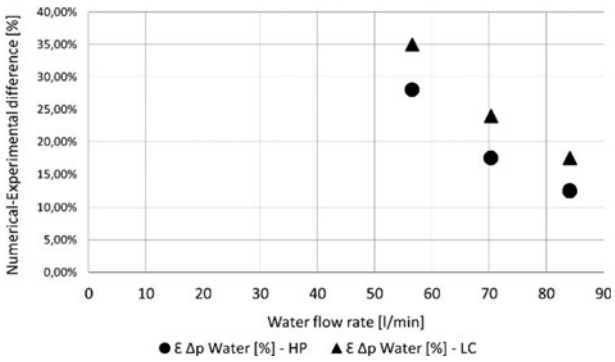

Figure 18. Percentage difference between numerical and experimental hot fluid pressure drop at different hot fluid (h.f.) flow rates.

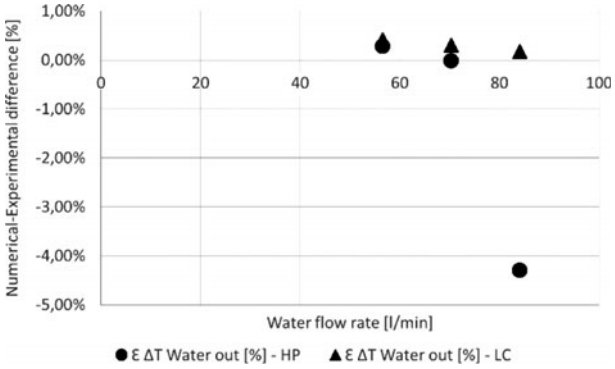

Figure 19. Percentage difference between numerical and experimental hot fluid output temp. at different h.f. flow rates.

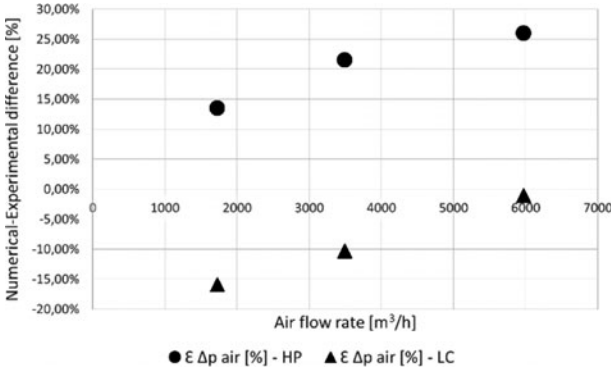

Figure 20. Percentage difference between numerical and experimental cold fluid pressure drop at different c.f. flow rates.

Nevertheless, the degree of approximation is similar to that obtainable with other techniques.

Figure 21 shows the percentage difference between experimental and calculated cold fluid output temperature. In this case, the correlation becomes again satisfactory, with an error between 2% and 8% for the HP geometry and between – 2% and 3% for the LC geometry. The HP geometry results show the most critical correlation.

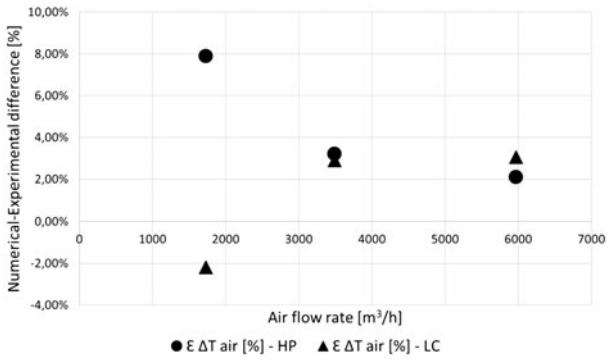

Figure 21. Percentage difference between numerical and experimental cold fluid output temp. at different c.f. flow rates.

6. Discussion

The differences between experimental and calculated results presented in Figure 17 and Figure 18 could be critically explained considering two aspects:

- At 56 l/min the flow velocity is 0.12 m/s and at 84 l/min is 0.76 m/s. The minimum flow velocity considered as boundary condition in the CFD analysis mapping is 0.2 m/s (see Table 2). This forces the software, at the lower flow rate, to extrapolate the calculation of exchanged power and pressure drop in a range of velocities external to the simulation range. The use of the mapping function outside the interval of data fitting naturally increases the calculation error. Further activity is needed to extend the mapping at working plane boundaries.
- In numerical simulations an ideal mixture (50% water – 50% ethylene glycol) was used. The experimental test rig could use pure water only. The two fluids (ideal mixture and pure water) differ in terms of constant pressure-specific heat (C_p) and kinematic viscosity as shown in Table 5.

According to Equation 11 the exchanged power is influenced by C_p, therefore, considering the data reported in Table 5, the software should underestimate the exchanged power compared to the experimental results. This behaviour is always shown by LC geometry, and only for the higher velocity (probably due to the extrapolation error) for the HP geometry.

Table 5. Properties of pure water and water - ethylene glycol mixture.

Properties at 70°C	Pure Water	Water – Ethylene glycol mixture (50% - 50%)
C_p (J/kg/K)	4191	3358
Kinematic Viscosity (cP)	404	950

On the other hand, the kinematic viscosity influences the Reynolds number.

$$Re = \frac{w \times D}{v} \tag{15}$$

For a generic circular tube the resistance coefficient is given by:

$$\lambda = \frac{64}{Re} \quad \text{laminar flow} \tag{16}$$

$$\lambda = \frac{0.3164}{Re^{0.25}} \text{ turbulent flow} \tag{17}$$

In all cases, the higher the kinematic viscosity the lower the Reynolds becomes, therefore the water – glycol mixture resistance coefficient increases compared to the pure water and the calculated pressure drop should overestimate the experimental results, as it found by experimental evidence.

About the air pressure drop, the discrepancy between numerical and experimental results could be reduced considering, in the CFD analysis, the air as *real gas* using, for example, the Virial state equation. This was not considered necessary at this stage.

In spite of the need for some criticism in some results, the overall validation procedure can be considered satisfactory, especially considering that the trends are confirmed in all cases and most of the discrepancies can be considered as results offset, indicating that an improvement in the CFD model could overcome the drawbacks. The effectiveness of the process, which starts from CFD results to the overall exchanger performance, is considered confirmed to this purpose.

7. Conclusion

The paper introduces the possibility to conceive a simplified methodology able to characterize the thermal and fluid-dynamic behaviour of a family of cross flow heat exchangers. The process was presented from a general point of view and applied to a practical case study, which starts from the analysis of five different cold flow and four different hot flow fins. The cold fluid is always air, the hot fluid is changed from air to water or oil. The generic radiator was divided into nine different sub-domain types which, after a preliminary study, were reduced to two. For each sub-domain a CFD model was developed and the pressure drop and the Wall Heat Transfer Coefficient (WHTC) calculated in nine different working points (3 flow rates and 3 temperatures). An overall number of 180 CFD simulation runs were performed in order to prepare maps of the predicted performance for each part. Considering that an average 50 cm heat exchanger, modelled at the same level of volume resolution in CFD mesh, at full scale would require more than 4 billion elements, and that this latter computation would be valid just for a single and unique size of heat exchanger, the benefits of the method proposed are significant.

A software tool, implementing the composition strategy described in the paper, was developed at IMAMOTER-C.N.R. Starting from the CFD results, and using cubic spline interpolations to fit the available data, the overall performance is estimated in a number of reference conditions. A set of experimental tests was carried out in view of procedure validation and assessment of confidence levels. Due to the test rig limitations, heat exchanger were tested in water-air case only. The obtained results indicated a good correlation between numerical and experimental data, especially when exchanged power and hot (cold) fluid output temperatures are considered. The pressure drop, in both hot and cold fluid case, shows a lower confidence level and have been critically reviewed. Considering that some of the differences can be explained in terms of limitations of the model, assumptions in the computation or differences between experimental conditions and numerical models, it is concluded that some improvements in the CFD model could lead to an even better match. In any case the application of the proposed procedure was considered feasible and improving existing design process.

Nomenclature

H_e	Height of heat exchanger	Z	Heat capacity rate
H_f	Height of fin sub-domian	ρ_H	Hot fluid density
H_s	Height of side	C_H	Hot fluid specific heat
H_t	Height of tube sub-domain	Q_H	Hot fluid flow rate
N_{Fl}	Number of fin layers	ρ_C	Cold fluid density
D_e	Depth of heat exchanger	C_C	Cold fluid specific heat capacity
L_{sF2}	Length of fin sub-domain (type 2)	Q_C	Cold fluid flow rate
L_{sF5}	Length of fin sub-domain (type 5)	h_e	Equivalent wall heat transfer coefficient
W_e	Width of heat exchanger	h_H	Hot fluid wall heat transfer coefficient
L_{sT2}	Length of tube sub-domain (type 2)	h_C	Cold fluid wall heat transfer coefficient
L_{sT5}	Length of tube sub-domain (type 5)	S_c	Cold fluid heat transfer surface
NTU	Number of Transfer Units	S_H	Hot fluid heat transfer surface
		T	Temperature

Acknowledgements

The authors would like to thank FIRA S.p.A. company for supporting and funding this work and the staff at the University of Bergamo, Italy, for their experimental activity.

Disclosure statement

The Authors of the paper declare that they did not had any financial interest or benefit arising from the application of their research.

Notes

1. This paper considers cross-flow heat exchangers only, however the extension of the procedure to different types is straightforward
2. This condition does not limit the validity and is directly applicable to arbitrary output pressure values.

Notes on Contributors

Dr. Roberto Paoluzzi Born in 1961 and MSc in Nuclear Engineering at the University of Bologna in 1986. Director of the Institute for Agricultural and Earth-Moving Machines (IMAMOTER) of the National Research Council of Italy (C.N.R.). Main research interests in fluid power systems and motion control technology, computational fluid dynamics and off-road machines design and safety. Chairman of ISO/TC 127/SC4, authored more than 300 technical papers and reports.

Dr. Antonino Bonanno MSc in Material Engineer at University of Messina in 2004. He received a Master degree in Fluid Power at University of Modena and Reggio Emilia in 2005. Researcher of the Italian National Research Council since 2005. He is involved in many research activities: innovative materials for fluid power applications, multi-body simulation, structural analysis, hydraulic circuits and heat exchanger study. He is also involved in International Standard activities under the Technical Committee ISO/TC 127. Author and coauthor of more than 30 scientific and technical papers.

Dr. Massimo Martelli Received the MSc. in Electronics Engineering from the University of Ferrara, Italy, in 2000. He is currently a researcher at the IMAMOTER institute (National Research Council of Italy). His main research interests are modelling and simulation of multi-domain systems (electrical + hydraulic + mechanical + thermal), aimed at system/component optimization and electronic control design and implementation, and multi-platform design of applications for advanced Human-Machine interaction, mainly applied to agricultural and earth-moving machines. He is also active on functional safety analysis, as a member of Project Group 2 of AEF (Agricultural industry Electronics Foundation). He is a author of more than 50 technical papers and reports.

Dr. Cristian Ferrari, PhD Received M.Sc. in Mechanical Engineering in 2008 and Ph.D. in Turbomachinery Design at University of Ferrara in 2012. From 2013 fellow Researcher at IMAMOTER Institute of the National Research Council of Italy. Worked on the study of hydraulic power transmission and computational fluid dynamics analysis. He is author of several papers and advisor of several master degree thesis.

References

Navarro, H.A. and Cabezas-Gòmez, L., 2005. A new approach for thermal performance calculation of cross-flow heat exchangers. *International Journal of Heat and Mass Transfer*, 48, 3880–3888.

Zarotti, G.L., 1998. Fluidi Oleodinamici – Nozioni e lineamenti introduttivi, CEMOTER-C.N.R. – Fluid Power Net.

Kim, M.H., Youn, B. and Bullard, C.W., 2001. Effect of inclination on the air-side performance of brazed aluminum heat exchanger under dry and wet conditions. *International Journal of Heat and Mass Transfer*, 44, 4613–4623.

Aslam Bhutta, M.M., et al., 2012. CFD applications in various heat exchangers design: a review. *Applied Thermal Engineering*, 32, 1–12.

Prasad, B.S.V., 1997. Fin efficiency and mechanism of heat exchange through fins in multi-stream plate-fin heat exchangers: development and application of a rating algorithm. *International Journal of Heat and Mass Transfer*, 40, 4279–4288.

Zhang, L.-Z., 2009. Flow maldistribution and thermal performance deterioration in a cross-flow air to air heat exchanger with plate-fin cores. *International Journal of Heat and Mass Transfer*, 52, 4500–4509.

Zhang, L., Yang, C. and Zhou, J., 2010. A distributed parameter model and its application in optimizing the plate-fin heat exchanger based on the minimum entropy generation. *International Journal of Thermal Sciences*, 49, 1427–1436.

Wen, J., et al., 2006. An experimental and numerical investigation of flow patterns in the entrance of plate-fin heat exchanger. *International Journal of Heat and Mass Transfer*, 49, 1667–1678.

Ismail, L.S., Ranganayakulu, C. and Shah, R.K., 2009. Numerical study of flow patterns of compact plate-fin heat exchangers and generation of design data for offset and wavy fins. *International Journal of Heat and Mass Transfer*, 52, 3972–3983.

Kim, M., Lee, K. and Song, S., 2008. Effect of pass arrangement and optimization of design parameters on the thermal performance of a multi-pass heat exchanger. *International Journal of Heat and Fluid Flow*, 29, 352–363.

Xie, G.N., Suden, B. and Wang, Q.W., 2008. Optimization of compact heat exchangers by genetic algorithm. *Applied Thermal Engineering*, 28, 895–906.

Hilbert, R., et al., 2006. Multi-objective shape optimization of heat exchanger using parallel genetic algorithms. *International Journal of Heat and Mass Transfer*, 49, 2567–2577.

Najafi, H., Najafi, B. and Hoseinpoori, P., 2011. Energy and cost optimization of plate and fin heat exchanger using genetic algorithm. *Applied Thermal Engineering*, 31, 1839–1847.

T'Joen, C., et al., 2010. Thermo-hydraulic study of a single row heat exchanger consisting of metal covered round tubes. *International Journal of Heat and Mass Transfer*, 53 (2010), 3262–3274.

McKinley, S. and Levine, M., 1999. Cubic Spline Interpolation, Math 45: Linear Algebra. Available from: http://online.redwoods.edu/instruct/darnold/laproj/Fall98/SkyMeg/Proj.PDF

Caratterizzazione a banco delle prestazioni di radiatori aria-acqua, 24 June 2012. University of Bergamo, Energy Systems and Turbomachinery Group, Final Report, private communication (in Italian)

ISO 5801:2007, Industrial fans — Performance testing using standardized airways.